Available online at www.sciencedirect.com
ScienceDirect
Nuclear Instruments and Methods in Physics Research B 260 (2007) 445–449
NIM B
Beam Interactions with Materials & Atoms
www.elsevier.com/locate/nimb

Porous silicon microcavities fabricated using ion irradiation

D. Mangaiyarkarasi [a,*], M.B.H. Breese [a], O.Y. Sheng [a], D.J. Blackwood [b]

[a] Department of Physics, 2 Science Drive 3, National University of Singapore, Singapore 117542, Singapore
[b] Department of Materials Science and Engineering, National University of Singapore, Singapore 117542, Singapore

Available online 14 February 2007

Abstract

By employing microcavity (MC) techniques, the broad spectral band and wide emission angle of photoluminescence from porous silicon (PSi) can be narrowed, directed and tuned in PSi microcavities. The microcavity structure is formed with a porous silicon active layer sandwiched between two Bragg reflectors. We have characterised the optical properties of the porous silicon multilayer structures. A number of Bragg reflectors and Fabry–Perot optical microcavities are fabricated with tuning of emission wavelengths over a wide range in heavily doped p-type silicon. The optical properties of these microstructures were investigated using reflectivity and photoluminescence measurements at different temperatures. This paper reports the ability of focussed 2 MeV proton beam irradiation to controllably blue shift the resonant wavelength of porous silicon microcavities in heavily doped p-type wafers. Using this process wafers are patterned on a micrometer lateral scale with microcavities tuned to different resonant wavelengths, giving rise to high-resolution full-colour reflection images over the full visible spectrum.

Keywords: PSi microcavity; Bragg reflectors; Photoluminescence; Ion irradiation

1. Introduction

1.1. Porous silicon microcavities

Visible light emission from the porous silicon (PSi) formed by anodic etching of Si in HF solution has attracted a great deal of research interest because it makes possible to produce a new generation of both active and passive optoelectronic devices [1,2]. Several efforts have been reported to demonstrate the quality and the intensity of electro and optical emission from PSi [3,4]. However, only limited improvements have been obtained in the practical device applications due to very broad spectral and angular emissions with aging effects [5]. The use of microcavity systems is a well-established tool to alter and control the spontaneous emission and has been realized in III–V semiconductor lasers [6–8]. Microcavities are formed by a layer structure similar to Fabry–Perot filter; a central active medium is embedded between two dielectric mirrors, which allow enhancement or inhibition of spontaneous emission at the energy of the cavity mode to be obtained, together with a highly directional emission [9]. Similarly, placing the porous silicon nanocrystals in a microcavity with dimensions comparable to optical wavelength reduces the spectral width of the photoluminescence spectrum of the active layer to the bandwidth of its resonant mode [10–12].

The mirrors of the microcavity and the active layer between them are fabricated with porous silicon, which has the ability to modulate its refractive index (n) between the indices of bulk silicon and air, simply by changing the porosity. Thus from the optical point of view, PSi can be described as a homogeneous mixture of silicon and air. To a first approximation, the optical constants of PSi vary with the relative Si and air content of the mixture (i.e. with porosity) according to the effective medium approximation [13–15]. By varying the applied current density (J), it is possible to change the porosity (percentage of void space) of the porous silicon film in the etching direction. Moreover

* Corresponding author.
E-mail address: phydm@nus.edu.sg (D. Mangaiyarkarasi).

0168-583X/$ - see front matter © 2007 Elsevier B.V. All rights reserved.
doi:10.1016/j.nimb.2007.02.061

the etching process is self-limited and the etching occurs only in the pore tips, so the porous layers already formed were not affected by the subsequent conditions of fabrication. Thus the porosity varies only with current density once the other etching parameters are kept constant, the formation of alternating PSi layers of different porosity (and hence different refractive index) results in dielectric multilayer structures that behave as optical interference filters, both in the infrared and visible wavelength ranges [16,17].

Several groups have already demonstrated the fabrication of PSi based Photonic band gap structures for many applications including DBRs and F–P filters [18–20], Rugate filters [21], microcavities with controlled spontaneous emission [22,23], waveguides [24,25] and color sensitive photodiodes [26]. Visible light emitting diodes based on PSi planar [27] and vertical [28] resonant cavities have been reported with tunable, narrow, and directional EL and PL spectral emissions [29]. Also random PSi multilayer structures [30] have been investigated theoretically and experimentally, since it is interesting in the field of one dimensional light localization. Recently, Reece et al. have reported the realization of optical microcavities with sub nanometer line widths at low temperature [31], whereas multiple narrow transmission peaks in a limited region of the stop band are observed in free standing PSi coupled optical microcavities by Ghulinyan et al. [32]. We have characterized the optical parameters for the porous silicon multilayer structure in 0.02 Ω-cm silicon and fabricated a number of high quality Bragg reflectors and Fabry–Perot optical microcavities with tuning of emission wavelengths over a wide range [33]. This paper reports the effect of ion irradiation on multilayers, which modifies the porous formation and hence the emission wavelength.

1.2. Effect of ion irradiation on porous silicon

Recently, we have performed focused high-energy ion beam irradiation studies on different resistivity p-type silicon to precisely control the emission characteristics of porous silicon [34–38]. A nuclear microprobe [39,40] was used to provide a focused 2 MeV proton beam to directly irradiate a desired pattern on silicon with micrometer resolution prior to electrochemical etching. The proton beam selectively creates lattice defects at the irradiated regions, where the porous formation occurs at a much reduced rate due to the increased resistivity during electrochemical etching. Low resistivity silicon (0.02 Ω cm) tends to produce PSi which emits low intensity PL due to excessive charge carrier concentration. At ion-irradiated regions, the increased local resistivity results in PSi which emits more intense PL due to the low carrier concentration than in substrate [36]. In contrast, higher resistivity silicon (1–10 Ω cm), usually exhibits efficient PL intensity, whereas ion irradiated regions produce red shifted PL in a controlled manner, with the shift depending on the ion dose [37,38]. We have extended these studies to investigate the effect of ion irradiation on porous silicon microcavity structures.

2. Results

2.1. Decrease in the thickness of the Bragg reflector at the irradiated regions

Lines of 2 μm wide and 2 mm long were irradiated with different doses of 2 MeV protons into 0.02 Ω cm p-type silicon as shown in Fig. 1(a). The 2 MeV ions lose energy as they penetrate the silicon and come to rest at a well defined range of ~50 μm. The stopping process damages the silicon lattice by creating additional defects, which locally reduce the concentration of free charge carriers. An electrical contact was made to the back surface of silicon using Ga–In eutectic and copper wire to allow a homogeneous current. Epoxy resin was used to protect the contact from HF. Anodization was performed at room temperature in a solution of $HF:H_2O:C_2H_5OH$ (1:1:2 by volume). A low porosity, L, (current density 10 mA/cm^2, time duration 4 s) and a high porosity H (100 mA/cm^2, 4 s) $\lambda/4$ layers were periodically repeated to form the distributed Bragg mirrors using computer controlled Keithely 220 programmable current/voltage source. Detailed procedures for the fabrication of the porous silicon Bragg reflectors and microcavities are

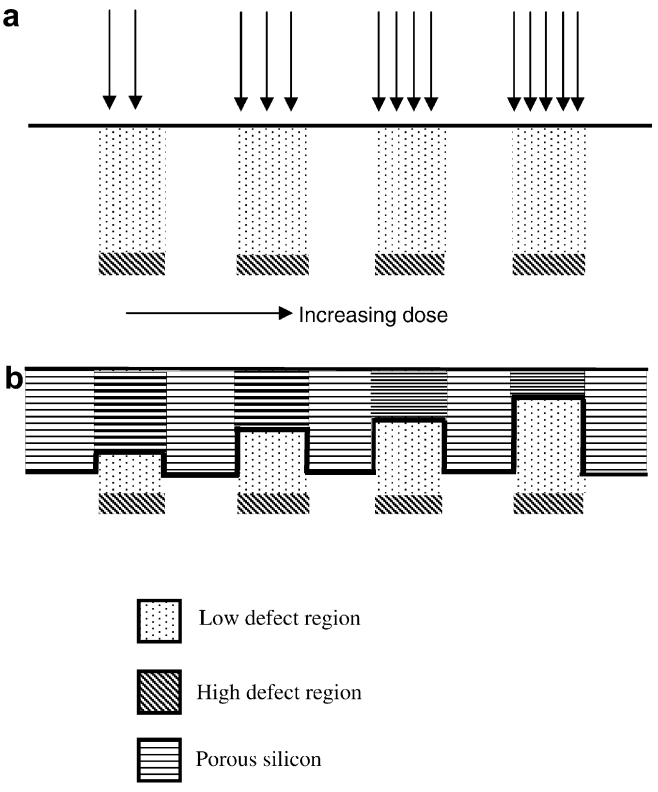

Fig. 1. Schematic representation of the effect of ion irradiation on formation of porous silicon Bragg reflectors (a) focused ion beam irradiation on p-type silicon with different doses, (b) electrochemical etching with alternating low and high current density to form Bragg reflector.

reported elsewhere [17]. Cross section scanning electron microscopy (SEM) analysis of these structures demonstrates the periodic variation of high and low porosity layers with smooth interfaces. Also it is found that the etching rate is progressively slowed at regions irradiated with larger doses, where ion-induced damage increases the resistivity with increasing dose resulting in reduced rate of hole current flowing through these regions during anodization. The schematic structure in Fig. 1(b) represents the evolution of the etching process across an irradiated boundary, exhibiting thinner porous layers, which is more pronounced with larger dose.

2.2. Ion induced changes in the optical properties of microcavities

Furthermore, we have investigated the ion-induced changes in the optical properties of Bragg reflectors and microcavities using reflectivity and photoluminescence measurements. A high resolution optical microscope (Nikon eclipse ME600) was used to image the reflectance and photoluminescence emission at the micrometer sized irradiated regions. Fig. 2 shows reflection and photoluminescence images of a microcavity sample where eight squares of $200 \times 200\ \mu m^2$ irradiated with 2 MeV protons

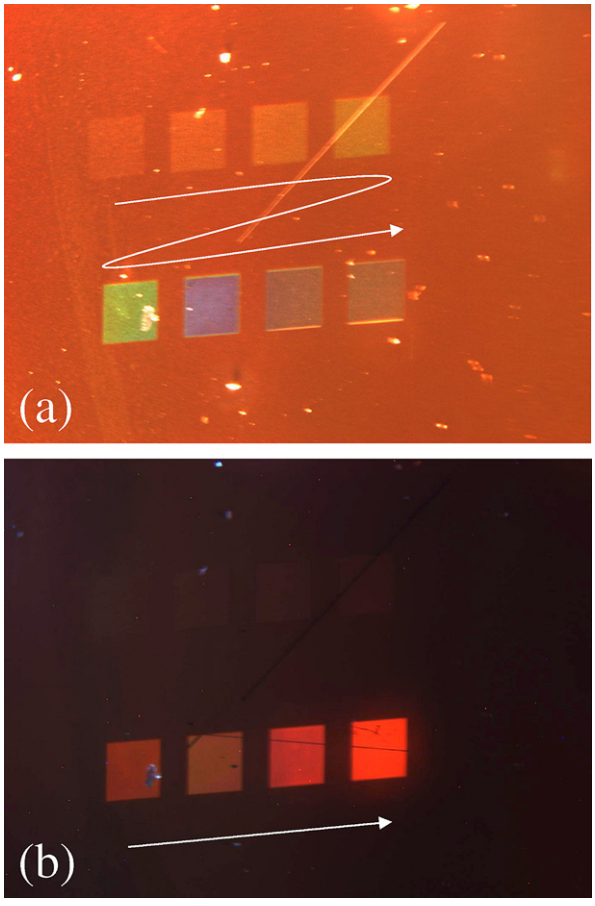

Fig. 2. (a) Optical, (b) photoluminescence images of $200 \times 200\ \mu m^2$ squares irradiated with 2 MeV protons over a wide range of doses.

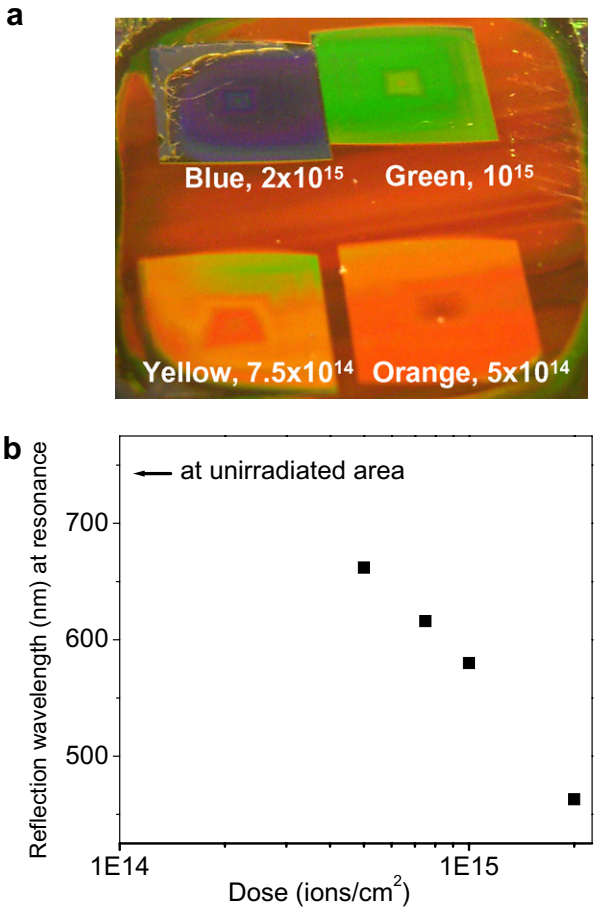

Fig. 3. (a) Photograph of a microcavity sample containing four squares of $3 \times 3\ mm^2$ irradiated with different doses. A range of colors are produced which are progressively blue shifted with increasing dose. (b) Shows the shift in the cavity resonance wavelength of the reflectivity spectra as a function of dose measured from the above irradiated squares. (For interpretation of color in this figure, the reader is referred to the web version of this article.)

over a wide range of doses. The microcavity consists of two 12 period Bragg mirrors with alternating high and low porosity layers all of which $\lambda/4$ thick etched at 40 and 75 mA/cm^2 respectively and a central active λ thick layer etched at 75 mA/cm^2, where λ is the wavelength at the cavity resonance. The etching times were chosen to form microcavity with resonant wavelength around 750 nm. Under illumination with white light, the reflected light from the unirradiated area shows reddish background, whereas from the irradiated squares, the reflectance gradually blue shifted with increasing dose. In the direction indicated by arrow in Fig. 2(a), starting with top left to right and again from bottom left to right, squares irradiated with increasing dose exhibits a range of reflected colors from yellow to violet[1]. Fig. 2(b) shows the PL image of the same regions captured under UV illumination. The PL intensity at the lowest four irradiated

[1] (For interpretation of color in this figure, the reader is referred to the web version of this article.)

Fig. 4. (a)–(c) Reflection images of 400×400 μm^2 regions irradiated with different overlaid scan patterns, corresponding to different doses to form dragon images. (d) Reflection image of miniature version of 'La Musique' painting (Henri Matisse) which was created by irradiating a 500×500 μm^2 area with different doses ranging from 4×10^{14} to 1.5×10^{15}/cm^2. In all cases the sample was illuminated with white light.

squares increases with increasing dose (in the direction indicated). Similar to earlier observation of the ion irradiation effect on porous silicon single layer [36], ion irradiation only enhances the PL emission at the microcavity formed irradiated regions, with no significant shift in the wavelength as compared to the reflection emission.

To investigate the optical behavior in more detail, microcavities with larger irradiated areas were prepared to perform the reflectance spectral measurements. Room temperature, normal-incidence reflectance spectra are recorded within the 3×3 mm^2 area of irradiated squares of different doses using UV–VIS–NIR spectrophotometer. We observed strong changes in the spectral response from the irradiated regions compared to the unirradiated background; first the reflectivity spectrum gradually shifts towards lower wavelengths as the dose increases as shown in Fig. 3(a). Fig. 3(b) shows the peak wavelength reflectance emission from the 3×3 mm^2-irradiated areas with doses ranging from 5×10^{14} to 2×10^{15} ions/cm^2. The cavity resonance wavelength from the unirradiated area is around $\lambda = 740$ nm, which has blue shifted to $\lambda = 490$ nm for a dose of 2×10^{15}/cm^2. Second, a dramatic reduction of the width ($\Delta\lambda$) of the reflectance spectrum has been observed in the irradiated regions with respect to unirradiated regions by a factor of 3. The observed blue shift in the reflected peak together with reduction in reflectance width on the irradiated areas probably owing to variations in the refractive index and layer thickness. It should be noted that the increased resistivity in the ion irradiation regions results in a reduction of layer thickness as discussed in Fig. 1. Furthermore, studies have been carried out to measure the variations in the refractive index and to explain the underlying mechanism in the narrowness of reflectance bandwidth and blue shift [41].

2.3. Full color reflection images from the ion irradiated porous silicon microcavity

We have adopted this approach to produce a wide range of tunable, controlled reflection emission wavelength from small, adjacent irradiated areas of porous silicon microcavities. Fig. 4(a)–(c) shows the optical reflection images of 400×400 μm^2 regions irradiated with different overlaid scan patterns, corresponding to different doses to form dragon images. Different portions in each image show different colors produced by different doses. Further, Fig. 4(d) demonstrates the versatility of our focused ion beam irradiation to reproduce a miniature version (500×500 μm^2) of the painting 'La Musique' by Henri Mattise by controllably patterning the wavelength of the reflected light from regions irradiated with doses ranging from 4×10^{14} to 1.5×10^{15}/cm^2. Slight variations in dose across an irradiated area result in different shifts of the central wavelength, hence slightly varying colors.

3. Conclusions

The optical properties of the ion irradiated Bragg reflector and microcavities have been investigated using reflectivity and photoluminescence measurements. The gradual

blue shift of the reflected peak wavelength with dose can be explained by the net reduction in the optical thickness of each porous layer. For full color display applications, this process could provide tunable, controlled reflection emission from adjacent micrometer size irradiated areas of porous silicon microcavities with utilizable efficiency across the whole visible range.

References

[1] L.T. Canham, Appl. Phys. Lett. 57 (1990) 1046.
[2] A.G. Cullis, L.T. Canham, Nature 353 (1991) 335.
[3] A. Givant, J. Shappir, A. Sa'ar, Appl. Phys. Lett. 73 (1998) 3150.
[4] G. Barillaro, A. Diligenti, F. Pieri, F. Fuso, M. Allegrini, Appl. Phys. Lett. 78 (2001) 4154.
[5] N. Koshida, H. Koyoma, Y. Yamanoto, G.J. Collins, Appl. Phys. Lett. 63 (1993) 2655.
[6] F. De Martini, G. Innocenti, G.R. Jacobovitz, P. Mataloni, Phys. Rev. Lett. 59 (1987) 2955.
[7] H. Yokoyama, K. Nishi, T. Anan, H. Yamada, S.D. Broson, E.P. Ippen, Appl. Phys. Lett. 57 (1992) 2814.
[8] A. Trdicucci, Y. Chen, V. Pellegrini, C. Deparis, Appl. Phys. Lett. 66 (1995) 2388.
[9] L. Pavesi, La Revista del Nuevo Cimento 20 (1997) 18.
[10] K.H. Li, D.C. diaz, Y. He, J.C. Campbell, C. Tsai, Appl. Phys. Lett. 64 (1993) 2655.
[11] P. Steine, F. Kozlowski, W. Lang, Appl. Phys. Lett. 62 (1993) 2700.
[12] L. Pavesi, M. Ceschini, G. Mariotto, E. Zanghellini, O. Bisi, M. Anderle, L. Calliari, M. Fedrizzi, J. Appl. Phys. 75 (1994) 1118.
[13] J.C. Maxwell-Garnett, Philos. Trans. R. Soc. London 203 (1904) 385.
[14] D.A.G. Bruggemann, Ann. Phys. 24 (1925) 636.
[15] H. Looyenga, Physica 31 (1965) 401.
[16] G. Vincent, Appl. Phys. Lett. 64 (1994) 2367.
[17] L. Pavesi, Microelectron. J. 27 (1996) 437.
[18] M.G. Berger, C. Dieker, M. Thonissen, L. Vescan, H. Luth, H. Munder, W. Theiss, M. Wernke, P. Goose, J. Phys. D: Appl. Phys. 27 (1994) 1333.
[19] C. Mazzoleni, L. Pavesi, Appl. Phys. Lett. 67 (1995) 2983.
[20] M. Araki, H. Koyama, N. Koshida, Jpn. J. Appl. Phys. 35 (1996) 2B 1041.
[21] M.G. Berger, M. Thonissen, R. Arens-Fischer, H. Munder, H. Luth, M. Arntzen, W. Theiss, Thin Solid Films 255 (1995) 313.
[22] L. Pavesi, C. Mazzoleni, A. Tredicucci, V. Pellegrini, Appl. Phys. Lett. 67 (1995) 3280.
[23] V. Pellegrini, A. Tredicucci, c. Mazzoleni, L. Pavesi, Phys. Rev. B 52 (1995) R14 328.
[24] A. Loni, L.T. Canham, M.G. Berger, R.A. fischer, H. Munder, H. Luth, H.F. Arrand, T.M. Benson, Thin Solid Films 276 (1996) 143.
[25] M. Araki, H. Koyama, N. Koshida, Appl. Phys. Lett. 68 (1996) 2999.
[26] M. Kruger, M. Marso, M.G. Berger, M. Thonissen, S. Billat, R. Loo, W. Reets, H. Luth, S. Hilbrich, R. Arens-Fischer, P. Grosse, Thin Solid Films 297 (1997) 241.
[27] L. Pavesi, R. Guardini, C. Mazzoleni, Solid State Commun. 97 (1996) 1051.
[28] M. Araki, H. Koyama, N. Koshida, Appl. Phys. Lett. 69 (1996) 2956.
[29] S. Chan, P.M. Fauchet, Appl. Phys. Lett. 75 (1999) 274.
[30] L. Pavesi, P. Dubos, Semicon. Sci. Technol. 12 (1997) 570.
[31] P.J. Reece, G. Lerondel, W.H. Zheng, M. Gal, Appl. Phys. Lett. 81 (2002) 4895.
[32] M. Ghulinyan, C.J. Oton, G. Bonetti, Z. Gaburro, L. Pavesi, J. Appl. Phys. 93 (2003) 9724.
[33] D. Mangaiyarkarasi, M.B.H. Breese, O.Y. Sheng, K. Ansari, C. Vijila, D.J. Blackwood, Proc. SPIE 6125 (2006) 61250X.
[34] M.B.H. Breese, E.J. Teo, D. Mangaiyarkarasi, F. Champeaux, A.A. Bettiol, D.J. Blackwood, Nucl. Instr. and Meth. B 231 (2005) 357.
[35] M.B.H. Breese, F.J.T. Champeaux, E.J. Teo, A.A. Bettiol, D.J. Blackwood, Phys. Rev. B 73 (2006) 035428.
[36] E.J. Teo, D. Mangaiyarkarasi, M.B.H. Breese, A.A. Bettiol, D.J. Blackwood, Appl. Phys. Lett. 85 (2004) 4370.
[37] D. Mangaiyarkarasi, E.J. Teo, M.B.H. Breese, A.A. Bettiol, D.J. Blackwood, J. Electrochem. Soc. 152 (2005) D173.
[38] E.J. Teo, M.B.H. Breese, A.A. Bettiol, D. Mangaiyarkarasi, F.J.T. Champeaux, F. Watt, D.J. Blackwood, Adv. Mater. 18 (2005) 51.
[39] M.B.H. Breese, D.N. Jamieson, P.J.C. King, Materials Analysis using a Nuclear Microprobe, Wiley, New York, 1996.
[40] M.B.H. Breese, G.W. Grime, M. Dellith, Nucl. Instr. and Meth. B 77 (1993) 332.
[41] D. Mangaiyarkarasi, M.B.H. Breese, O.Y. Sheng, C. Vijila, Appl. Phys. Lett. 89 (2006) 021910.